Analyst

RSC Publishing

PAPER

View Article Online
View Journal | View Issue

Cite this: *Analyst*, 2013, **138**, 2032

Aptamer-aided target capturing with biocatalytic metal deposition: an electrochemical platform for sensitive detection of cancer cells

Zi Yi, Xiao-Yan Li, Qing Gao, Li-Juan Tang* and Xia Chu*

Received 12th October 2012
Accepted 12th January 2013

DOI: 10.1039/c3an36474g

www.rsc.org/analyst

A novel aptamer biosensor for cancer cell assay has been reported on the basis of ultrasensitive electrochemical detection. Cancer cell capturing is first accomplished *via* aptamer-aided recognition, and the cell–aptamer binding events then mediate an alkaline phosphatase-catalyzed silver deposition reaction which can be probed by electrochemical detection. Following biocatalytic silver deposition, an efficient amplification approach for sensitive electrochemical measurements is demonstrated, for cell detection with high sensitivity. Ramos cell are used as a model case, a typical biomarker of the acute blood cell cancer, Burkitt's lymphoma. The results reveal that the developed technique displays desirable selectivity in Ramos cell discrimination, and linear response range from 10 to 10^6 cells with a detection limit as low as 10 cells. Due to the simple procedures, label-free and electrochemistry based detection format, this technique is simple and cost-effective, and exhibits excellent compatibility with miniaturization technologies. The electrochemical cell detection strategy may create an intrinsically specific and sensitive platform for cancer cell assay and associated studies.

Introduction

Cancers are among the most harmful diseases for humans. Due to their genetic abnormalities, cancer cells usually exhibit abnormal behavior at molecular level, which causes ~7 million people die of cancers every year.[1,2] Hence, the detection of cancer cells has emerged as a central problem in cancer diagnosis, especially for early clinical diagnosis.[3,4] In the past, various strategies for cancer cell detection have been reported, such as immunocytochemical methods,[5–7] cytometric methods,[8,9] and polymerase chain reaction (PCR)-based methods.[10–13] Although these methods have had some success in cancer cell detection, many suffer from costly labeled reagents, time-consuming operations, or sophisticated instrumentation. Therefore, the development of simple, low-cost methods with high sensitivity and selectivity for the detection of cancer cells is still a high requirement.

Recently, novel aptamer biosensors were reported for cell detection.[3,14–16] Aptamers are short single-stranded oligonucleotides and they are usually highly specific to certain targets.[17–19] Compared with conventional biomolecular ligands such as antibodies, an aptamer may exhibit prominent advantages in site-specific labeling, structure-controlled design, and by its easy and reproducible production. These properties make aptamers an ideal molecular recognition tool for biomedical detection and biosensor developments. Aptamer-based biosensors can be developed using various signal readout techniques, such as quartz crystal measurement,[20,21] optical measurement[22–24] and electrochemical measurement.[25–30] Electrochemical methods have received considerable attention because of the high sensitivity, low cost, and excellent compatibility with miniaturization technologies. With the development of signal amplification techniques that can be further employed to improve the performance of electrochemical methods, an electrochemical biosensor holds great potential as a next-generation molecular detection strategy for cancer cells. However, few efforts have been made as yet in the development of an electrochemical biosensor for cell detection using biocatalytic metal deposition, a demonstrated technique with excellent performance in signal amplifying.[31–36]

Motivated by our previous observations on biocatalytic metal deposition in sensitive enhancement,[31–33,36] we report a proof-of-principle novel electrochemical aptamer biosensor technique for cancer cell detection based on enzyme-catalyzed silver deposition. The strategy combines a biphasic architecture with specific aptamer-aided cell recognition followed by ultrasensitive electrochemical detection of the product of the metal deposition reaction close to the electrode. Because aptamers have high fidelity in target recognition, it allows the developed strategy to be highly specific in cancer cell detection. Enzyme-catalyzed silver deposition provides an efficient amplification approach to electrochemical measurements, thus, can offer cell

State Key Laboratory of Chemo/Bio-Sensing and Chemometrics, College of Chemistry and Chemical Engineering, Hunan University, Changsha, 410082, P. R. China. E-mail: tanglijuan@hnu.edu.cn; xiachu@hnu.edu.cn; Fax: +86-731-88821916; Tel: +86-731-88821916

detection at high sensitivity. In addition, aptamers can be prepared by chemical synthesis and be readily used without further modification, making the assays effortless and cost-efficient. To demonstrate this strategy, Ramos cell line is used, a typical biomarker of the acute blood cell cancer, Burkitt's lymphoma. The developed strategy may create a convenient and cost-efficient platform for the detection of cancer cells with high sensitivity and selectivity.

Experimental

Reagents and materials

Bovine serum albumin (BSA) and streptavidin–alkaline phosphatase (SA–ALP) were purchased from Dingguo Biotechnology Co. Ltd. (Beijing, China). Ascorbic acid 2-phosphate was purchased from Express Technology Co., Ltd. (Japan). NaCl, KH_2PO_4, Na_2HPO_4, Tris–HCl, EDTA, NaOH, glycine, $AgNO_3$, and KNO_3 were of analytical purity and obtained from the Sinopharm Chemical Reagent Co. Ltd. (Shanghai, China). All the other solutions were prepared using ultrapure water (>18 MΩ) produced by a Millipore Milli-Q water purification system (Billerica, MA, USA).

The synthesized oligonucleotides, all HPLC-purified and lyophilized, were provided by Takara Biotech. Co. Ltd. (Dalian, China). The sequence for capture aptamer probe **1** was 5′-SH–TTTTTTTTTTCACCGGGAGGATAGTTCGGTGGCTGTTCAGGGTC TCCTCCCGGTG-3′, and for aptamer probe **2** was 5′-biotin–TTTTTTTTTTTAGGCAGTGGTTTGACGTCCGCATGTTGGGAATA GCCACGCCT-3′. These were the aptamers for Ramos cells.[4] Thermodynamic parameters and secondary structures of both oligonucleotides were calculated using bioinformatics software (http://mfold.rna.albany.edu/). Ramos cells (CRL-1596, B-cell, human Burkitt's lymphoma) and human serum were kindly provided by Hunan Provincial Tumor Hospital.

Cell culture and cell treatment

The cells were cultured in RPMI medium supplemented with 10% fetal bovine serum (FBS) and 100 IU per mL penicillin–streptomycin at 37 °C in humidified air containing 5% CO_2, and were kept in logarithmic growth phase by routine passage every 2–3 days. Then, they were collected, centrifuged at 1800 rpm for 3 min, and washed twice with a 10 mM PBS (100 mM NaCl, pH 7.4). The sediments were then resuspended in 0.01 M PBS or in human serum to obtain cell suspension. The cell number was determined by using a Petroff-Hausser cell counter.

Gold electrode treatment and capture aptamer immobilization

Gold disc electrodes (~2 mm diameter, 99.99% polycrystalline, CH Instrument Inc.) were treated with Piranha solution (H_2SO_4/H_2O_2 = 3 : 1 in volume) for 3 h, polished with 0.05 μm gamma alumina suspension (CH Instrument Inc.) for 5 min, and then sonicated in ultrapure water and ethanol for 3 min twice to remove bond particles. Then, the electrode was rinsed thoroughly with ultrapure water and dried under mild nitrogen flow. 7 μL solution containing 1 μM thiol group modified capture aptamer probe **1** in10 mM Tris–HCl buffer (1 M NaCl, pH 8.0) was added on the pretreated gold electrode for 12 h at 4 °C. The electrode surface was then rinsed with 10 mM PBS buffer (pH 7.4) containing 100 mM NaCl for 10 min, and dried in a nitrogen gas stream.

Aptamer-aided cell capture

10 μL sample prepared by dispersing a certain amount of target cells in 0.01 M PBS was added on the surface of a gold electrode where captured aptamer **1** had been immobilized, and incubated at 37 °C for 1 h. Then, the electrode was rinsed thoroughly with 0.01 M PBS for 10 min and dried under mild nitrogen flow. Subsequently, a 7 μL of 3 μM aptamer probe **2** was added on the surface of the gold electrode and incubated at 37 °C for 1 h to form a sandwich complex of thiolated aptamer–cell–biotinylated aptamer. To avoid a nonspecific interaction of SA–ALP with the gold electrode, 7 μL of 5% BSA solution was added on the surface of a gold electrode and incubated at 37 °C for 30 min, followed by rinsing the electrode with 0.01 M PBS for 10 min.

Enzyme-catalyzed silver deposition and electrochemical detection

Later, 7 μL 100 μg mL^{-1} SA–ALP was dispensed to the prepared gold electrode, and incubated for 1 h at 37 °C. After rinsing using 0.01 M PBS (pH 7.4), the gold electrode was immersed in a 50 mM freshly prepared glycine–sodium hydroxide buffer (pH 9.08) containing 1 mM $AgNO_3$ and 1 mM ascorbic acid 2-phosphate, and incubated at 37 °C for 30 min. The resulting electrode was rinsed with ultrapure water.

Electrochemical measurements including linear sweep voltammetry (LSV) and electrochemical impedance spectroscopy (EIS) were performed on an electrochemical analyzer CHI-660A (CH Instruments, Shanghai, China) at room temperature (~25 °C). A three-electrode system consisting of a KCl saturated calomel reference electrode (SCE), a platinum counter electrode and the working electrode (gold electrode) was used. LSV was performed at a potential range from 0.1 to 0.8 V (*vs.* SCE) with a 100 mV s^{-1} scan rate in a 0.6 M KNO_3 solution containing 0.1 M HNO_3. EIS was performed in 1/15 M PB (pH 7.4) containing 5 mM $Fe(CN)_6^{3-}$/$Fe(CN)_6^{4-}$ (1 : 1 mixture) and 0.1 M KCl in the frequency range from 0.1 Hz to 100 KHz at a bias potential of −0.19 V (*vs.* SCE) with frequency modulation of 5 mV.

The images of silver nanoparticles deposited on the gold electrode were measured by Scanning Electron Microscope (SEM, JSM-6700F, Japan).

Results and discussion

Analytical principle of the electrochemical sensor

The analytical principle of the electrochemical aptamer biosensor is illustrated in Fig. 1. Two aptamer probes with different sequences and binding sites of the same cancer cell are designed. Aptamer probe **1** is thiolated at the 5′ end and *via* covalent binding, its thiolated end can be immobilized onto the surface of the gold electrode. Aptamer **2** is a probe biotinylated

at its 5′ end. These two probes, **1** and **2**, both have 10 thymine bases on their 5′ ends to maintain proper spatial comformations and thus promote the binding efficiency.[37]

In typical assays, the thiolated probe **1** immobilized on the surface of working electrode, which is also the aptamer for the target cell, recognises and specifically captures the target cell close to the electrode. In the presence of probe **2**, another aptamer for the target cell, it further specifically binds with the captured cancer cell. As probe **2** is biotinylated, it can conjugate with the SA–ALP through the biotin–streptavidin interaction. Thus, it allows the nonreductive substrate of alkaline phosphatase, ascorbic acid 2-phosphate, to be converted into reducing agent ascorbic acid on the electrode surface. Hence, the silver ions are reduced and deposited on the electrode surface. Note that the specific bindings are achieved only with aptamer probes for the target cells. Therefore, SA–ALP mediated silver deposition can only occur in the presence of target cell, and the targets can be instantly determined by the metallic silver reduced electrochemical signal. Furthermore, as the aptamer sensor utilizes the enzymatic silver deposition procedure for electrochemical quantification of the target cell, it permits the accumulation of the enzymatic product at the electrode surface for a highly sensitive LSV readout.

Typical characteristics of cancer cell detection

For a biosensor developed using the aptamers of Ramos cell based on the strategy described in the present study, Fig. 2A depicts its typical LSV response curves for the detection of different cancer cells, Ramos cell as the target and CEM cell for the control. The electrochemical signals were recorded after 10 μL sample solutions (10^5 cells per μL) incubated with 7 μL probe **2** (3 μM) at 37 °C for 1 h, and the subsequent enzymatically deposition of silver for 30 min on the surface of probe **1** (7 μL, 1 μM) modified gold electrode. For CEM cells, a signal as low as that obtained in the absence of any cell was observed (~0.82 μA). In contrast, a well-defined peak corresponding to silver stripping was observed at ~0.45 V *versus* SCE for Ramos cell, with a sharp increase of 8.93 μA in the oxidation peak current. The increased current implied a successful deposition of metal silver on the surface of the electrode. As the significant peak current increase caused by deposited silver can only be achieved in the presence of the target cells, it indicates that the developed aptamer sensor is highly specific in cancer cell detection. This may benefit from the intrinsically high affinities of aptamers. The differences between the gold electrode surface before or after enzymatic silver deposition was also investigated using SEM. As shown in Fig. 2B, compared with the electrode surface observed before the procedure of enzymatic silver deposition, a much rougher surface was obtained after the enzymatic silver deposition step. It can be seen that silver nanoparticles were randomly decorated on the electrode surface (Fig. 2B(b)), proof of the successful deposition of metal silver on the surface of the gold electrode.

To investigate the surface interactions, electrochemical impedance measurements using Ramos cells and their

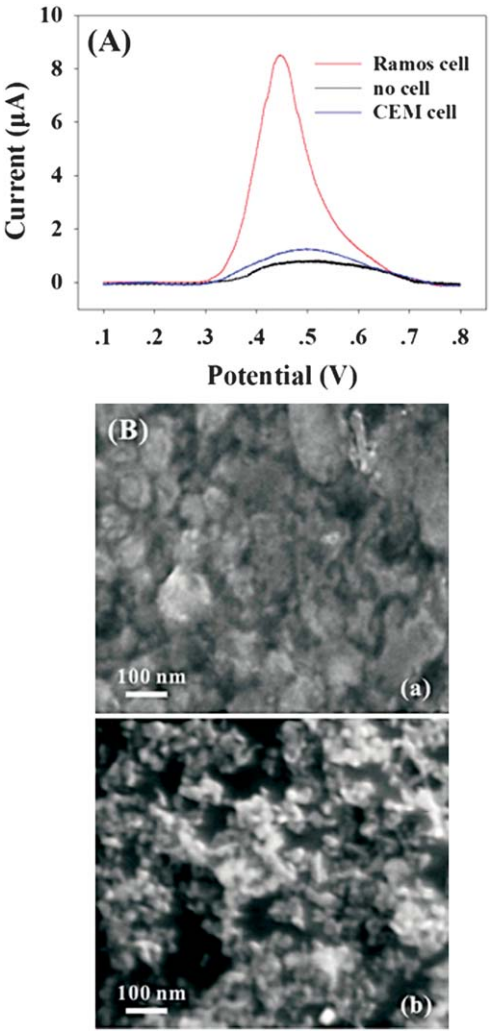

Fig. 2 (A) LSV curves obtained in the assay of different cells. Scanning was performed in 0.6 M KNO_3/0.1 M HNO_3 from 0.1 to 0.8 V. 10 mM PBS containing 0.1 M NaCl (pH 7.4) was used as the reaction buffer. (B) SEM images of the gold electrode surface before (a) or after (b) enzymatic silver deposition obtained in the assay of Ramos cells.

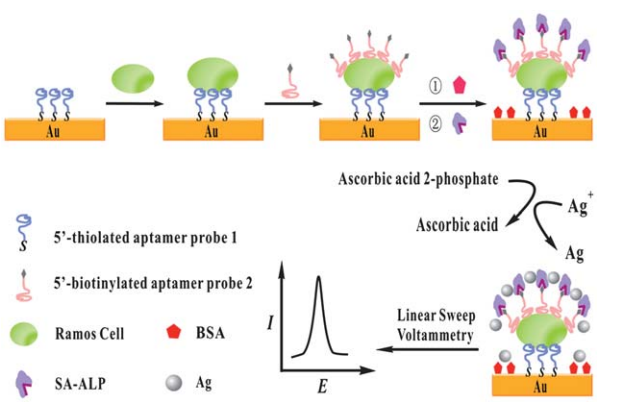

Fig. 1 Schematic diagram of electrochemical cell detection based on aptamer-aided cell capture followed by biocatalytic metal silver deposition close to the surface of electrode.

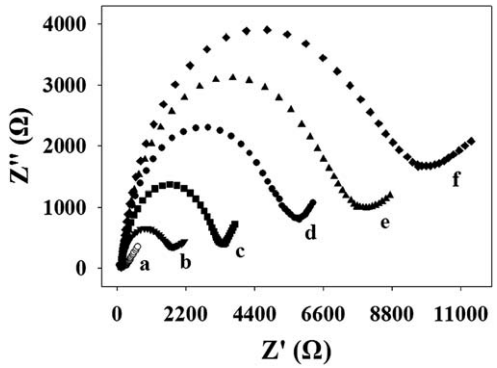

Fig. 3 Nyquist plot for electrochemical impedance measurements in PBS buffer (10 mM, pH 7.4) containing 5 mM $Fe(CN)_6^{3-/4-}$ (1 : 1 mixture) as the redox probe at 0.24 V for (a) bare gold electrode; (b) probe **1**–gold electrode; (c) Ramos cells–probe **1**–gold electrode; (d) probe **2**–Ramos cells–probe **1**–gold electrode; (e) BSA–probe **2**–Ramos cells–probe **1**–gold electrode; (f) SA–ALP–BSA–probe **2**–Ramos cells–probe **1**–gold electrode. Frequency range: 0.1 to 100 kHz; ac amplitude, 5 mV.

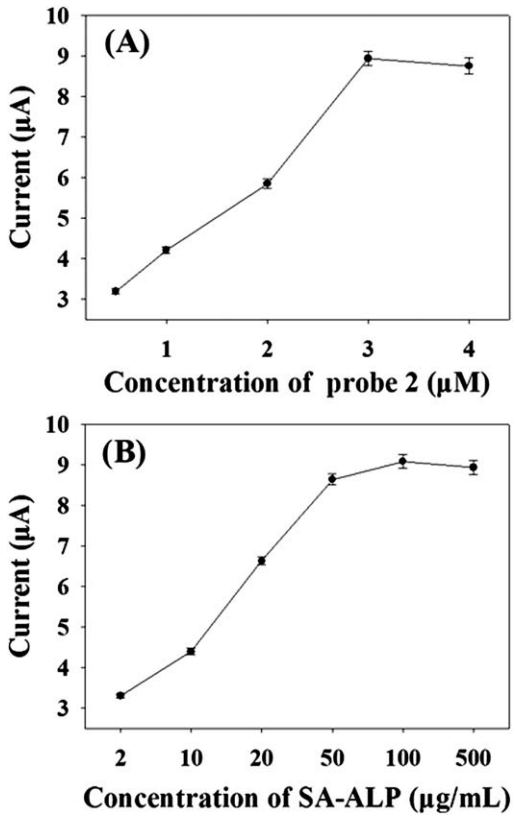

Fig. 4 Dependency of LSV signals on the concentration of probe **2**(A) or SA–ALP (B), obtained by incubating 10 μL sample solutions (10^6 Ramos cells per μL). The error bars represent RSD across three repetitive experiments.

corresponding aptamer probes were performed. The impedance spectra in the form of a Nyquist plot in the investigation was obtained (Fig. 3). One can observe that the bare gold electrode behaved as an ideal conductor and the impedance spectra gave a linear plot (curve a). The oligonucleotide-modified electrode exhibited a much larger impedance than the bare electrode

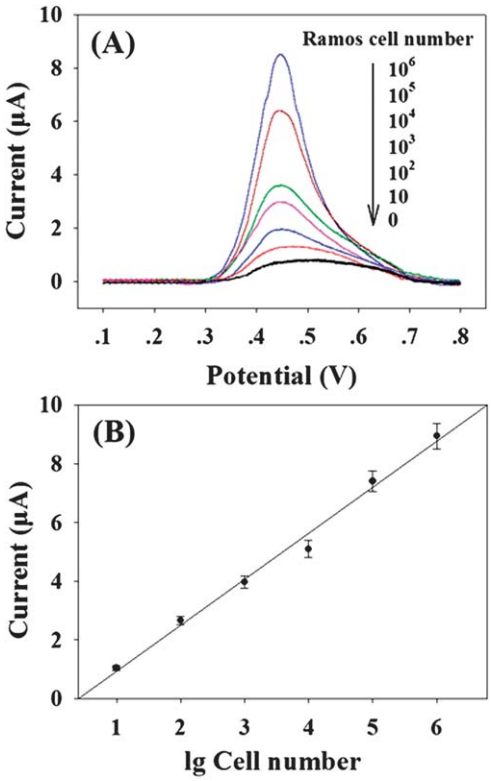

Fig. 5 (A) Typical LSV curves obtained *via* surface silver deposition in response to target Ramos cell of varying amounts in 10 μL sample solution. (B) Corresponding LSV peak currents *versus* target Ramos cell amounts. LSV was recorded in 0.6 M KNO_3/0.1 M HNO_3 from 0.1 to 0.8 V (*vs.* SCE). The error bars represent RSD across three repetitive experiments.

(curve b), due to the formation of a barrier for the electron transfer at the electrode interface. After incubating with Ramos cells, the impedance of the electrode further increased (curve c), indicating binding of Ramos cells to the aptamer probe **1** immobilized on the electrode surface. With the treatment of biotinylated probe **2**, BSA and SA–ALP conjugates, the electrode gave much larger impedance (curves d–f). These provide immediate evidence of surface binding events.

Optimization of experimental conditions

For the developed biosensor, biotinylated probe **2** specifically binded with the captured Ramos cells first and then conjugated with the SA–ALP on the surface of the working electrode, so the performance of the biosensor was highly dependent on the concentration of probe **2**. The concentration of SA–ALP conjugates that mediated the metal silver deposition also had a great impact on the performance of the biosensor. Fig. 4 depicts typical LSV responses in correlation to the two assay conditions. It was observed that with the increasing concentration of probe **2**, LSV peak current intensities in assay of Ramos cells were enhanced substantially at first, and then became flat when the concentration was larger than 3 μM. Therefore, the concentration of probe **2** was used throughout subsequent experiments. For SA–ALP conjugates, a similar trend was obtained in LSV signals, peak current intensity gradually increased with

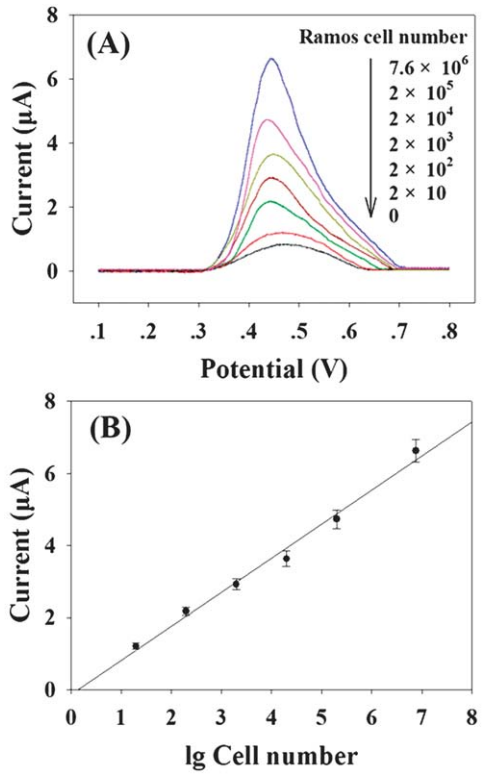

Fig. 6 (A) Typical LSV curves obtained *via* surface silver deposition in response to target Ramos cell of varying amount in 10 μL human serum solution. (B) Corresponding LSV peak currents *versus* target Ramos cell amounts in human serum. LSV was recorded in 0.6 M KNO_3/0.1 M HNO_3 from 0.1 to 0.8 V (*vs.* SCE). The error bars represent RSD across three repetitive experiments.

increasing concentration and levelled off with concentrations up to 100 μg mL^{-1}. Thus, the concentration of SA–ALP conjugate was used throughout subsequent experiments. In addition, the concentrations of 1 mM $AgNO_3$ and 1 mM ascorbic acid 2-phosphate have been chosen as optimal concentrations according to the work previously reported by our group.[38]

Quantitative analysis of cancer cells

Under the optimal detection conditions (1 μM aptamer probe **1**, 3 μM aptamer probe **2**, 100 μg mL^{-1} SA–ALP, 10 mM PBS containing 0.1 M NaCl, pH 7.4), we investigated the performance of the developed electrochemical aptamer sensor in quantitative analysis of cancer cells. Fig. 5A depicted typical LSV response curves of the samples (10 μL) with varying amounts of Ramos cells. A dynamic increase in peak current intensity was observed with increasing target cell amounts within the range from 10 to 10^6. A high-dose sensitivity was also obtained in this five-decade cell number range with a detection limit as low as 10 Ramos cells, an amount readily available in cancer cell detection. Compared with the sensors reported by other groups,[39–41] the developed sensor exhibited a relatively high sensitivity for the detection of Ramos cells. Additionally, the present strategy possessed excellent reproducibility. Relative standard deviations (RSDs) of peak current intensities were 4.9%, 3.2% and 4.3% in three repetitive assays of 10^2, 10^4 and 10^6 Ramos cells. The stability of the sensor was also studied under continuous linear scans for 10 cycles, and the results indicated that the developed sensor had excellent stability. The response time of the sensor for the detection of Ramos cells was about 3 h, which was relatively short compared to existing methods for the detection of Ramos cells. In addition, it may be cost-efficient and easily automated because of the relatively simple operation procedures and label-free electrochemical detection format.

Detection of Ramos cells in human serum

To further demonstrate the feasibility of the developed biosensor, it was used for the analysis of cancer cells in biological fluids. A series of human serum samples containing different amounts of Ramos cells were prepared and the corresponding current intensities wererecorded (Fig. 6). A dynamic increase in peak current intensity was observed with increasing target cell amounts in human serum within the range from 20 to 7.6 × 10^6 with a detection limit of 20 Ramos cells. The sensitivity for the detection of Ramos cells in human serum was almost the same as that for the detection of Ramos cells in PBS, clearly revealing that the developed biosensor may become a promising technique for cancer cell assay.

Conclusion

A novel electrochemical aptamer biosensor was developed for cancer cell detection based on aptamer-aided cell recognition followed by biocatalytic metal silver deposition on the surface of the electrode. The use of aptamers provide this technique with good specificity for identification of cancer cells, and the utilization of enzymatic silver deposition allows highly efficient amplification of cell capturing events. Using Ramos cell line as a model case, the developed strategy was demonstrated to display high selectivity in discriminating Ramos cells, detection limit as low as 10 cells, and a wide linear response range 10 to 10^6 cells with desirable reproducibility. Due to its label-free and electrochemical-based detection format, the technique may prove to be cost-efficient with excellent compatibility to miniaturization technologies. These properties support its potential in clinical applications. Moreover, multiplex detection of multiple cells can be implemented in densely packed array format with specific aptamers selected for each kind of cell. In view of these advantages, this new electrochemical cell detection strategy is expected to provide an intrinsically specific and sensitive platform for cancer cell assay and associated studies.

Acknowledgements

This work was supported by the National Natural Science Foundation of China (No. 20975035, 21275045), NCET-11-0121, and Hunan Provincial Natural Science Foundation of China (Grant 12JJ1004).

References

1 A. Jemal, T. Murray, E. Ward, A. Samuels, R. C. Tiwari, A. Ghafoor, E. J. Feuer and M. J. Thun, *Ca-Cancer J. Clin.*, 2005, **55**, 10–30.

2 Y. F. Huang, H. T. Chang and W. H. Tan, *Anal. Chem.*, 2008, **80**, 567–572.
3 C. D. Medley, J. E. Smith, Z. W. Tang, Y. R. Wu, S. Bamrungsap and W. H. Tan, *Anal. Chem.*, 2008, **80**, 1067–1072.
4 G. D. Liu, X. Mao, J. A. Phillips, H. Xu, W. H. Tan and L. W. Zeng, *Anal. Chem.*, 2009, **81**, 10013–10018.
5 M. P. Osborne, G. Y. Wong, S. Asina, L. J. Old, T. J. Cote and P. P. Rosen, *Cancer Res.*, 1991, **51**, 2706–2709.
6 A. A. Ross, B. W. Cooper, H. M. Lazarus, W. Mackay, T. J. Moss, N. Ciobanu, M. S. Tallman, M. J. Kennedy, N. E. Davidson and D. Sweet, *Blood*, 1993, **82**, 2605–2610.
7 J. Y. Pierga, C. Bonneton, A. Vincent-Salomon, P. D. Cremoux, C. Nos, N. Blin, P. Pouillart, J. P. Thiery and H. Magdelenat, *Clin. Cancer Res.*, 2004, **10**, 1392–1400.
8 S. Koizumi, M. Konishi, T. Ichihara, H. Wada, H. Matsukawa, K. Goi and S. Mizutani, *Eur. J. Cancer*, 1995, **31A**, 1682–1688.
9 X. F. Che, Y. Nakajimaa, T. Sumizawa, R. Ikeda, X. Q. Ren, C. L. Zheng, M. Mukai, T. Furukawa, M. Haraguchi, H. Gao, Y. Sugimoto and S. I. Akiyama, *Cancer Lett.*, 2002, **187**, 111–119.
10 R. A. Ghossein and S. Bhattacharya, *Eur. J. Cancer*, 2000, **36**, 1681–1694.
11 M. King, W. Su, A. Chang, A. Zuckerman and G. W. Pasternak, *Nat. Rev. Neurol.*, 2001, **4**, 268–274.
12 T. Illmer, M. Schaich, U. Oelschlagel, R. Nowak, U. Renner, B. Ziegs, S. Subat, A. Neubauer and G. Ehninger, *Leuk. Res.*, 1999, **23**, 653–663.
13 S. A. Ahrendt, J. T. Chow, L. H. Xu, S. C. Yang, C. F. Eisenberger, M. Esteller, J. G. Herman, L. Wu, P. A. Decker, J. Jen and D. Sidransky, *J. Natl. Cancer Inst.*, 1999, **91**, 332–339.
14 T. Deng, J. S. Li, L. L. Zhang, J. H. Jiang, J. N. Chen, G. L. Shen and R. Q. Yu, *Biosens. Bioelectron.*, 2010, **25**, 1587–1591.
15 J. E. Smith, C. D. Medley, Z. W. Tang, D. H. Shangguan, C. Lofton and W. H. Tan, *Anal. Chem.*, 2007, **79**, 3075–3082.
16 Y. Xu, J. A. Phillips, J. L. Yan, Q. G. Li, Z. H. Fan and W. H. Tan, *Anal. Chem.*, 2009, **81**, 7436–7442.
17 S. Centi, S. Tombelli, M. Minunni and M. Mascini, *Anal. Chem.*, 2007, **79**, 1466–1473.
18 R. Kirby, E. J. Cho, B. Gehrke, T. Bayer, Y. S. Park, D. P. Neikirk, J. T. McDevitt and A. D. Ellington, *Anal. Chem.*, 2004, **76**, 4066–4075.
19 K. M. You, S. H. Lee, A. Im and S. B. Lee, *Biotechnol. Bioprocess Eng.*, 2003, **8**, 64–75.
20 M. Liss, B. Petersen, H. Wolf and E. Prohaska, *Anal. Chem.*, 2002, **74**, 4488–4495.
21 S. Tombelli, M. Minunni and M. Mascini, *Biosens. Bioelectron.*, 2005, **20**, 2424–2434.
22 W. A. Zhao, W. Chiuman, M. A. Brook and Y. F. Li, *ChemBioChem*, 2007, **8**, 727–731.
23 R. A. Potyrailo, R. C. Conrad, A. D. Ellington and G. M. Hieftje, *Anal. Chem.*, 1998, **70**, 3419–3425.
24 X. N. Zhang, Y. Q. Teng, Y. Fu, L. L. Xu, S. P. Zhang, B. He, C. G. Wang and W. Zhang, *Anal. Chem.*, 2010, **82**, 9455–9460.
25 G. S. Bang, S. Cho and B. G. Kim, *Biosens. Bioelectron.*, 2005, **21**, 863–870.
26 H. M. So, K. Won, Y. H. Kim, B. K. Kim, B. H. Ryu, P. S. Na, H. Kim and J. O. Lee, *J. Am. Chem. Soc.*, 2005, **127**, 11906–11907.
27 J. A. Hansen, J. Wang, A. N. Kawde, Y. Xiang, K. V. Gothelf and G. Collins, *J. Am. Chem. Soc.*, 2006, **128**, 2228–2229.
28 K. Ikebukuro, C. Kiyohara and K. Sode, *Biosens. Bioelectron.*, 2005, **20**, 2168–2172.
29 C. Y. Tong, B. X. Shi, X. J. Xiao, H. D. Liao, Y. Q. Zheng, G. L. Shen, D. Y. Tang and X. M. Liu, *Biosens. Bioelectron.*, 2009, **24**, 1777–1782.
30 D. K. Xu, D. W. Xu, X. B. Yu, Z. H. Liu, W. He and Z. Q. Ma, *Anal. Chem.*, 2005, **77**, 5107–5113.
31 Y. Tan, X. Chu, G. L. Shen and R. Q. Yu, *Anal. Biochem.*, 2009, **387**, 82–86-.
32 L. Zhou, L. J. Ou, X. Chu, G. L. Shen and R. Q. Yu, *Anal. Chem.*, 2007, **79**, 7492–7500.
33 B. Qu, X. Chu, G. L. Shen and R. Q. Yu, *Talanta*, 2008, **76**, 785–790.
34 Z. P. Chen, Z. F. Peng, Y. Luo, B. Qu, J. H. Jiang, X. B. Zhang, G. L. Shen and R. Q. Yu, *Biosens. Bioelectron.*, 2007, **23**, 485–491.
35 H. Cai, Y. Q. Wang, P. G. He and Z. Fang, *Anal. Chim. Acta*, 2002, **469**, 165–172.
36 P. Zhang, X. Chu, X. M. Xu, G. L. Shen and R. Q. Yu, *Biosens. Bioelectron.*, 2008, **23**, 1435–1441.
37 S. M. Schreiner, D. F. Shudy, A. L. Hatch, A. Opdahl, L. J. Whitman and D. Y. Petrovykh, *Anal. Chem.*, 2010, **82**, 2803–2810.
38 Z. P. Chen, Z. F. Peng, Y. Luo, B. Qu, J. H. Jiang, X. B. Zhang, G. L. Shen and R. Q. Yu, *Biosens. Bioelectron.*, 2007, **23**, 485–491.
39 G. D. Liu, X. Mao, J. A. Phillips, H. Xu, W. H. Tan and L. W. Zeng, *Anal. Chem.*, 2009, **81**, 10013–10018.
40 C. D. Medley, J. E. Smith, Z. W. Tang, Y. R. Wu, S. Bamrungsap and W. H. Tan, *Anal. Chem.*, 2008, **80**, 1067–1072.
41 G. F. Jie, L. Wang, J. X. Yuan and S. S. Zhang, *Anal. Chem.*, 2011, **83**, 3873–3880.